Boundary Lubrication, Hemifusion, and Self-Healing of Binary Saturated and Monounsaturated Phosphatidylcholine Mixtures

Boundary Lubrication, Hemifusion, and Self-healing of Binary Saturated and Monounsaturated Phosphatidylcholine Mixtures ♦

Yifeng Cao, Nir Kampf, and Jacob Klein*

Department of Materials and Interfaces, Weizmann Institute of Science, Rehovot 76100, Israel

*Jacob.klein@weizmann.ac.il

♦ We dedicate this paper to the memory of Jacob Israelachvili, a great scientist and a path-breaking pioneer in the measurement and understanding of surface interactions.

Abstract

A wide range of phosphatidylcholine (PC) lipids with different degrees of unsaturation has been identified in the human synovial fluid and on the cartilage surface. The outstanding lubricity of the articular cartilage surface has been attributed to boundary layers comprising complexes of such lipids, though to date only lubrication by single-component PC-lipid-based boundary layers has been investigated. As distinguishable lubrication behavior has been found to be related to the PC structures, we herein examined the surface morphology (on mica) and the lubrication ability of binary PC lipid mixtures, 1,2-dipalmitoyl-*sn*-glycero-3-phosphocholine (DPPC) and 1-palmitoyl-2-oleoyl-*sn*-glycero-3-phosphocholine (POPC), using atomic force microscopy (AFM) and a surface force balance (SFB). These two PC lipids are among the most abundant saturated and unsaturated PC components in synovial joints. Small unilamellar vesicles (SUVs) prepared from DPPC-POPC mixtures (8:2, 5:5, and 2:8, molar ratios) ruptured and formed bilayers on mica. The normal and shear forces between two DPPC-POPC bilayer-coated mica surfaces across the corresponding SUV dispersions show good boundary lubrication (friction coefficients $\leq$ ca. 10^{-4}) up to contact stresses of 8.3 ± 2.2 MPa for 8:2 DPPC-POPC and 5.0 ± 1.7 MPa for the others. Hemifusion induced at high normal pressures was observed, probably because of the height mismatch of two components. Reproducible successive approaches after hemifusion indicate rapid self-healing of the mica-supported bilayers in the presence of the SUVs reservoir. This work is a first step to provide insight concerning the lubrication, wear, and healing of the PC-based boundary layers – which must consist of multicomponent lipid mixtures - on the articular cartilage surface.

Keywords: Phosphatidylcholine (PC) lipids, hydration lubrication, binary lipid mixtures, self-healing bilayers, boundary lubricants

■ INTRODUCTION

Phosphatidylcholine (PC) is the major class of phospholipid (PL) present in biological systems.[1,2,3] PC molecules consist of a zwitterionic phosphocholine headgroup and two hydrophobic alkyl chain tails. As surface-active compounds, PC lipids participate in many biological activities at interfaces, such as lubrication in the articular joints and preventing adhesion in the peritoneal cavity.[4,5,6] The remarkable lubrication ability of the articular joint, with low kinetic friction coefficients (0.03 – 0.001) at pressures up to 5 – 10 MPa or more,[7,8,9] has attracted much interest due to the increasing demand for treating osteoarthritis and designing lubricating biomaterials.

Inspired by nature, the lubricating ability of PC lipids has been investigated. The most abundant saturated PC in synovial fluid, 1,2-dipalmitoyl-*sn*-glycero-3-phosphocholine (DPPC), has been widely studied as a model PC lubricant for natural and artificial joint[10,11] and biomaterials[12,13] under aqueous conditions. Results show that DPPC is capable of reducing friction and protecting the substrate from wear at room temperature.[9,10,11,12] A further study shows that the lubrication behavior of DPPC is temperature-dependent: more pronounced decrease in shear force was observed at temperature above the main solid-ordered (or gel) to liquid-disordered (or liquid crystalline) phase transition temperature (T_m).[14]

The lubrication behavior of different PC lipids is greatly related to the phase states of PC lipids,[15,16] which is determined by the length and degree of unsaturation of alkyl chains. Generally, PCs with shorter alkyl chain lengths or unsaturated tails have lower T_m than experimental room temperature (25 ^{o}C). For these PC lipids in the liquid disordered state, the tails are more randomly oriented and the bilayers are loosely packed.

Such a fluid bilayer allows reduced friction coefficients between two bilayers supported by hard quartz or mica substrates, self-healing from the lipid reservoir;[6,15] but cannot maintain such good lubricating ability under high pressures when supported by mica or hyaluronic acid (HA) layer under water or aqueous salt solutions (no lipid reservoir).[17,18]

Extremely low friction coefficients under physiological pressures (up to ca. 100 atm) have been achieved by PC lipids in robust solid-ordered (gel) state with or without a lipid reservoir, and for PC lipids in their fluid liquid crystalline state in dispersion, as measured by the surface force balance (SFB).[15,17] The lubrication mechanism is attributed to the hydration lubrication effect: the water molecules bind to the zwitterionic headgroups via dipole-charge interactions and at the same time exchange rapidly with free water molecules. This leads to strong hydration repulsion upon close approach and reduced energy dispassion when two surfaces slide pass each other, and consequently provides low friction coefficients.[16,19,20,21] This general mechanism also accounts for lubrication by hydrated ions,[19,21,22] charged surfactants,[23] and zwitterionic polymer brushes[24] under aqueous solutions.

In contrast to PC lipids which are able to offer extreme lubrication under physiological pressures, the biomacromolecules in the articular joint, such as hyaluronic acid (HA), lubricin, and aggrecan, cannot by themselves provide comparable lubrication ability.[25,26] A proposed scenario for articular joint lubrication is that the synergistic effect of HA, lubricin and PC lipids together play a key role, in which the PC lipids in the outer layer, exposing their highly-hydrated phosphocholine groups, are responsible for reducing the friction coefficient.[18,27,28] The PC identified in the joint, however, is composed of a wide range of lipids with different acyl chain lengths and degrees of

unsaturation.[2,3,29] Particularly, up to 86.0 ± 6.5 mol% of total PCs in human synovial fluid are unsaturated and ~ 61.38% of the PC alkyl chains on the cartilage surface bear one or more unsaturated bonds.[3,30] While lubrication by boundary layers consisting of single-component PC lipids, including DPPC and 1-palmitoyl-2-oleoyl-*sn*-glycero-3-phosphocholine (POPC), have been examined, clearly in joints such boundary layers must consist of mixtures of the different lipids. Thus, understanding the roles of gel-state saturated PC lipids and liquid crystalline-state unsaturated ones in binary mixtures, and the correlation between physical properties and interfacial interactions of binary saturated and unsaturated PC lipids, are an important first step for better understanding the biolubrication mechanism and further designing efficient PC-based boundary lubricants.

In this work, we evaluated the boundary lubricating performance of mixtures of DPPC and POPC (structures shown in Figure 1), the most abundant saturated and unsaturated PCs identified in synovial fluid and on the cartilage surface.[2,3] SUVs prepared from DPPC-POPC mixtures were characterized by lipid composition, size distribution, surface zeta potential, and main T_m. The studied DPPC-POPC mixtures includes a gel-state DPPC-rich mixture (8:2), a fluid-state POPC-rich mixture (2:8), as well as a mixture of equal molar ratios (5:5). The morphology of SUVs adsorbed on mica was characterized by atomic force microscopy. The normal and shear forces between two opposing mica surfaces coated with DPPC-POPC-SUVs fused bilayers were measured across SUV dispersions using an SFB. Based on the results, the lubrication behavior of DPPC-POPC mixtures were evaluated.

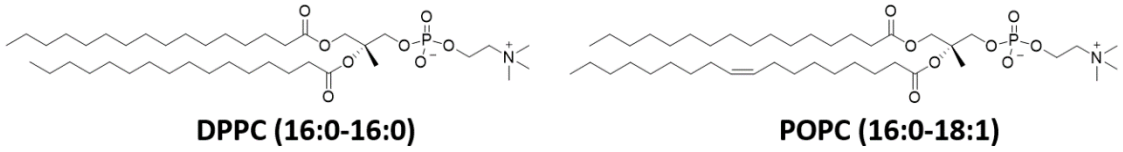

Figure 1. Chemical structures of DPPC and POPC.

■ EXPERIMENTAL SECTION

Materials. DPPC and POPC lipids with purities > 99.5 wt.% were purchased from Lipoid GmbH (Ludwigshafen, Germany). Water was purified through a Thermo Scientific™ Barnstead™ GenPure™ water purification system, with a resistivity of 18.2 MΩ·cm and the total organic carbon content ≤ 1 ppb. This study is carried out in water with no added salt, in future work we will probe the effect of physiological level salt concentrations.

Preparation of Liposomes. Mixed DPPC-POPC powders were prepared by dissolving suitable amounts of both PC lipids in chloroform/methanol (3/1, v/v) at a final concentration of ~ 100 mg lipids/mL solvent, well mixed by vortexing, dried by blowing N_2 overnight, and then lyophilized overnight. The obtained mixture was then mixed with water, sonicated in a water bath at 50 ˚C (above the phase transition temperatures of DPPC 41 ^{o}C and POPC -2 ^{o}C) for 5 min and vortexed for 5 min to get well dispersed multilamellar vesicles (MLVs). After that, the MLV dispersions were downsized to achieve a uniform size distribution by extruding under pressure through polycarbonate membranes with pore sizes of 0.4 μm, 0.1 μm, and 0.05 μm for 5, 10, and 12 times, respectively. The temperature of the extruder was kept at 50 ^{o}C by a water circulation bath connected to the extruder jacket. The prepared liposome dispersions were cooled down to room temperature and stored at 4 ˚C before use within 24 hours.

Dynamic Light Scattering (DLS). Size distribution and zeta-potential (ζ) of liposome dispersions were measured on a Malvern's Zetasizer Nano ZSP instrument at 25 ^{o}C and measurements were at a backscatter angle of 173˚.

Atomic Force Microscopy (AFM). The morphology of adsorbed SUVs on mica surface was characterized by AFM, which was carried out on an Asylum MFP-3D SA instrument. Silicon tip on nitride lever with a nominal spring constant of 0.35 N·m^{-1} (SNL, Bruker) was used for imaging. Samples were prepared by incubating freshly cleaved mica, which was firmly glued inside a petri dish, in 0.3 mM liposome dispersions for more than 2 hours. Unless specified, scans were done with non-contact mode under 0.3 mM liposome dispersion.

Surface Force Balance (SFB). The normal ($F_n(D)$) profiles and shear (F_s) forces as well as the absolute surface separation D between two mica surfaces were measured with SFB, the details of which were explained in previous work.[23,31] Briefly, the single-crystal mica (ruby muscovite, Grade 1, S&J Trading Inc., NY) facets of 2.5 - 3.2 μm thickness were back-silvered and glued onto hemi-cylindrical quartz lenses using epoxy resin (EPON Resin 1004F, Miller-Stephenson Chemical Co., Inc.). Two lenses were amounted onto upper and lower holders in a cross-cylinder configuration. The separation between two surfaces (D) was calculated from the wavelength of fringes of equal chromatic order (FECO) compared with the mica in contact,[32] with an accuracy of ± 0.3 nm. The normal force was measured in a quasi-static approach and calculated according to the bending of the normal spring (spring constant k_n = 127 N/m). The shear force $F_{s,measure}$ was calculated according to the bending of a set of vertical springs (spring constant k_s = 300 N/m) via an air-gap capacitor (Accumeasure ASP-1-ILA, MTI Instrument, NY) as a response to a

lateral back-and-forth movement applied to the upper lens by a piezoelectric probe. The shear forces (F_s) was calculated by $F_s = F_{s,measure} - F_{s,0}$, where $F_{s,0}$ was the (low) systematic signal measured at $D > 500$ nm. The maximal lateral displacement with our SFB is ca. 2 μm, and a range 0.2 – 2 μm lateral displacement was applied. Since the lateral contact dimension is around 10 μm, this means that around 2% - 20% 'new' area is probed when a 0.2 – 2 μm lateral motion is applied. Friction coefficients (μ) were calculated by the ratios of F_s to F_n at the highest pressure P_{max} measured in each force profile. The P_{max} was calculated by the maximum F_n divided by the contact area A, ($A = \pi \cdot a^2$, where a is half the flattened width of the fringe). The interfacial tension (γ) was calculated according to the Johnson-Kendall-Roberts (JKR) theory by the equation $\gamma = F_{pull\text{-}off}/3\pi R$, where $F_{pull\text{-}off}$ was calculated by the product of jump-out distance and the normal spring constant, and R was the mean radius of curvature.[33] The experiment was conducted at 25 ± 0.5 ^{o}C in a temperature-stabilized room. Data listed for each DPPC-POPC system were obtained from two independent experiments, with a number of independent contact points in each.

Unless specified, 0.8 mL of 6 mM SUV dispersion was introduced to the boat filled with ~ 16 mL water. The final concentration of PC lipids in the boat was ca. 0.3 mM, in with the range of the total phospholipid concentration in human synovial fluid.[30] Measurements were performed after more than two hours incubation in SUV dispersion.

■ RESULTS AND DISCUSSION

Liposome Characterization

Liposomes prepared from mixed DPPC and POPC of three molar ratios, 8:2, 5:5 and 2:8, were characterized by DLS, zeta-potential, NMR, and DSC. The size distribution of prepared liposomes was ~ 70 nm and the PDI values were less than 0.1 (Supplementary Information, SI, Table S1), indicating that uniformly distributed SUVs were prepared by the extrusion.[34] The zeta-potential (ζ) values of the prepared liposomes were all close to zero (see Table S1), as expected for the zwitterionic PC phosphocholine headgroups. The DPPC to POPC molar ratios in the prepared SUVs were evaluated from the NMR spectra (Figure S1), which also revealed that there was no detected hydrolysis of PC to lysophosphatidylcholine.[35] DSC measurements (Figure S2) show hysteresis for the main phase transition temperatures (T_m) of all single- and binary-component SUVs, similar to the observation of PC-MLVs and -LUVs.[36] The T_m values upon heating (cooling) are estimated to be 35.0 (34.3), 29.3 (28.8), and 2.0 (0.0) ^{o}C for DPPC-POPC 8:2, 5:5, and 2:8, whereas those for DPPC- and POPC-SUVs are 40.7 (39.6) and -2.9 (4.9) ^{o}C, respectively.

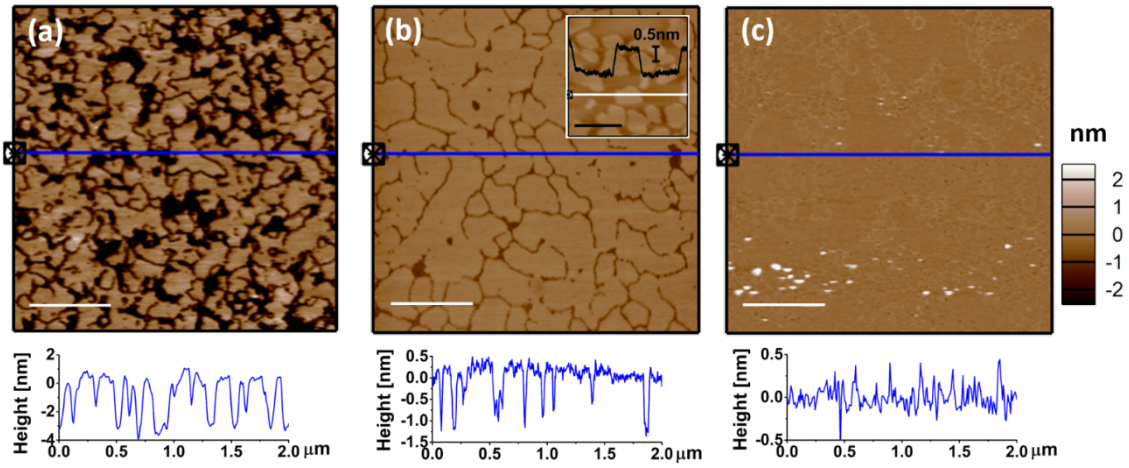

Figure 2. AFM images (2 µm × 2 µm) of DPPC-POPC-SUVs prepared from DPPC-POPC molar ratios of 8:2 (a), 5:5 (b), and 2:8 (c) adsorbed on freshly cleaved mica. The

images (a) and (b) were obtained after 4 h incubation, while image (c) was after 2 h incubation. Equilibrium was reached for all the three systems, indicated by the unchanged morphology at different scanning areas. Inset image in (b) (500 nm × 500 nm) shows morphology of mica-supported bilayer after 1.5 h incubation in 0.3 mM DPPC-POPC-SUV 5:5 dispersion. The dots in image (c) are extra materials attached to the bottom layer. All the scans were done under 0.3 mM SUV dispersion at room temperature (~ 25 ^{o}C). The scale bar for images (a-c) is 500 nm, and for the inset image in (b) is 200 nm.

The morphology of DPPC-POPC-SUVs adsorbed on mica was characterized by AFM scanning under an SUV dispersion. As seen in Figure 2, the SUVs ruptured and formed continuous lipid bilayer on freshly cleaved mica surfaces, which was further confirmed by SFB according to the limiting thickness (~ 5 nm), or 'hard-wall', reached at the highest compressions attained. For the DPPC-POPC 8:2 system (Figure 2a), phase separation between thicker (DPPC-rich) and thinner (POPC-rich) domains was observed even after equilibrium, which is in agreement with a previous study.[37] For the other two systems, line defects, possibly corresponding to borders of adjacent domains,[38] also exist, and small-area phase separation is observed for DPPC-POPC 5:5 (Figures 2b-c, Figure S3). As mica surface is negatively charged under aqueous environment, the single-component PC-SUVs adsorb on mica mainly through the mica-charge vs. zwitterionic-dipole interactions,[18] and form closely packed vesicles (gel-state PC) or supported bilayer (liquid-crystalline state PC), depending on the phase state of PC lipid.[16,27] In the DPPC-POPC system, the POPC-rich domains with lower van der Waals interaction between the tails cause the rupture of liposomes. This is in agreement with a previous finding that the liquid crystalline state PC in a mixture with a gel state one plays a more important role in liposome rupture on a hydrophilic substrate.[39]

Normal forces

Approaching force profiles. The profiles of normal-force versus distance between two opposing mica surfaces across 0.3 mM DPPC-POPC-SUV dispersions (following their incubation for 4 hours in the dispersion) are presented in Figures 3a-c. For the three systems, a similar trend was observed. As the two surfaces approached from more than 500 nm, there was no detected interaction above the scatter at surface separations $D >$ ca. 100 nm. Weak repulsion ($F_n > 0$) commenced from c.a. 100 nm, and significant repulsion (> 1 mN m^{-1}) was observed from ~ 40 nm. This repulsive interaction range is shorter than that between negatively charged mica surfaces (~ 200 nm) bearing single-component gel-state DSPC- or DPPC-SUVs (~ 100 nm), but similar to the cases of liquid crystalline-state POPC-SUVs.[15,40] Considering that the zwitterionic headgroups are polar and the surface of the prepared SUVs is electroneutral, this weak repulsion is most likely steric in origin and caused by expelling excess liposomes, loosely-attached on top of the lipid bilayers, out of the contact region.[15,17]

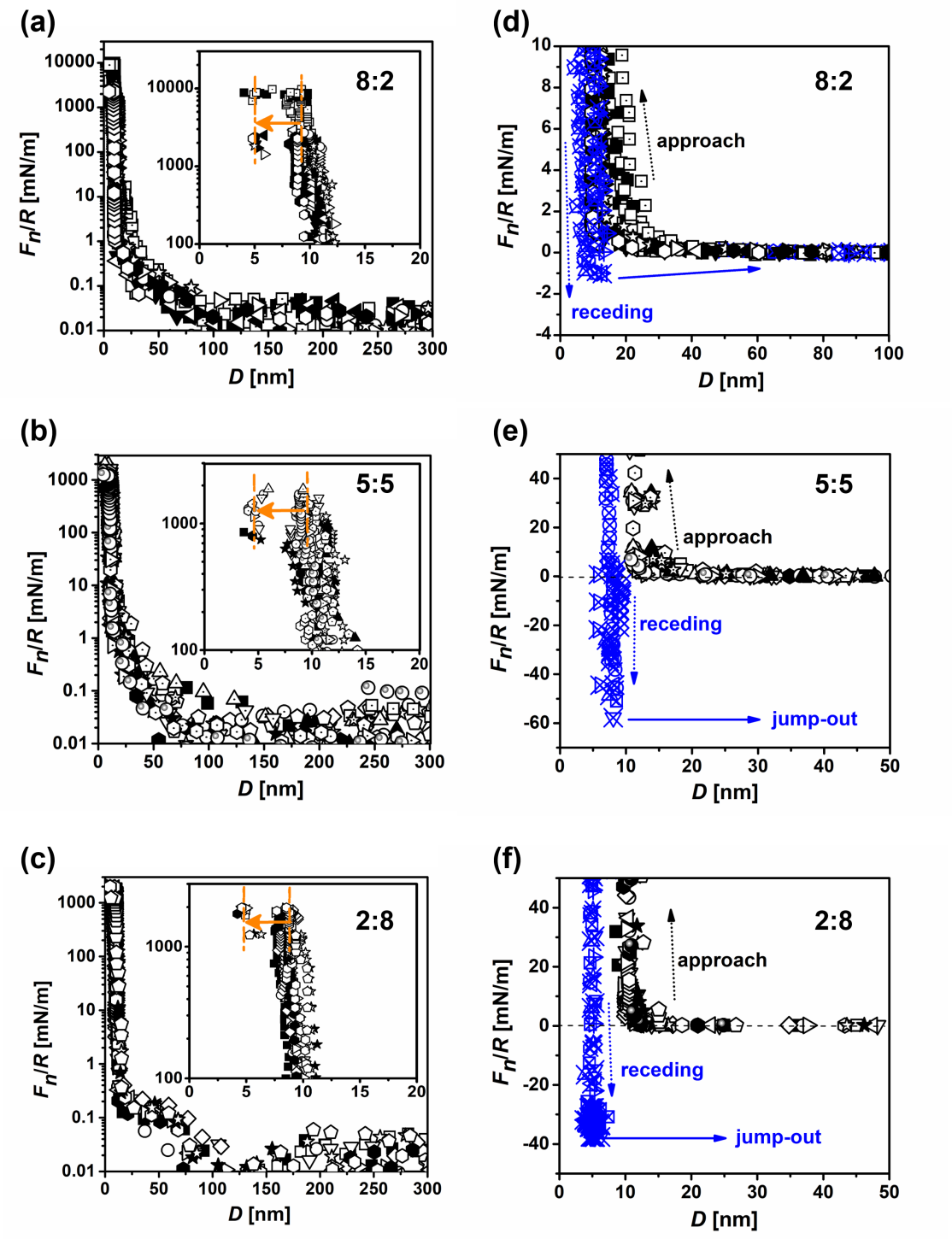

Figure 3. Normal forces (F_n) normalized by the radius of curvature (R) versus separation distance (D) for DPPC-POPC 8:2 (a and d), 5:5 (b and e) and 2:8 (c and f) immersed in 0.3 mM of the respective DPPC-POPC-SUV dispersions. The filled symbols represent the first approaches at different contact positions, while the empty/empty-with-dot ones

represent the successive approaches. In (d-f), The crossed symbols were obtained from the receding profiles and the solid lines with arrow indicate 'jump-out'.

At strong compression the repulsive force increased as *D* decreases to a 'hard-wall' separation of 9.3 ± 0.8, 8.7 ± 1.1, and 8.5 ± 0.5 nm as the molar ratio of POPC increases in the order of DPPC-POPC 8:2, 5:5, and 2:8. As the thicknesses of fully hydrated DPPC and POPC bilayers are 4.7 nm[41] and 3.9 nm[42], the observed values are between two bilayers of DPPC and of POPC, corresponding to two DPPC-POPC mixed bilayers. The flat tips of the fringes (Figure 4, upper images in a and b) indicate that two bilayers without any extra materials remained in the contact area. Such strong, short-ranged repulsive force between two facing PC bilayers, according to previous studies, are hydration repulsion arises mainly from the hydration layers coating the zwitterionic headgroups.[43]

When the normal force/pressure reached a certain critical point, 'jump-in' phenomena indicating decreases in the distance between the two surfaces were observed (see insets in Figures 3a-c). For DPPC-POPC 5:5, *D* decreases from 8.7 ± 1.1 nm to 4.6 ± 0.6 nm at pressures of 5.0 ± 1.7 MPa, and for the 2:8 system, *D* reduces from 8.5 ± 0.5 nm to 4.6 ± 0.2 nm at pressures of 5.0 ± 0.5 MPa. The change in distance and the flat fringe tips before and after 'jump-in' (Figures 4a-b) indicate that one bilayer was squeezed out of the whole contact area, namely, full hemifusion took place.[44] This hemifusion is a rapid process which lasts less than 1s. For the DPPC-POPC 8:2 system, however, a stage appeared in the flattened tip of the fringe (Figure 4a, bottom image), where the distance between two mica surfaces decreased from 9.3 ± 0.8 nm to a final

distance 5.3 ± 0.7 nm in this stage at normal pressure up to 8.3 ± 2.2 MPa. These results indicate that partial hemifusion occurred in the contact region (Figure 4a).

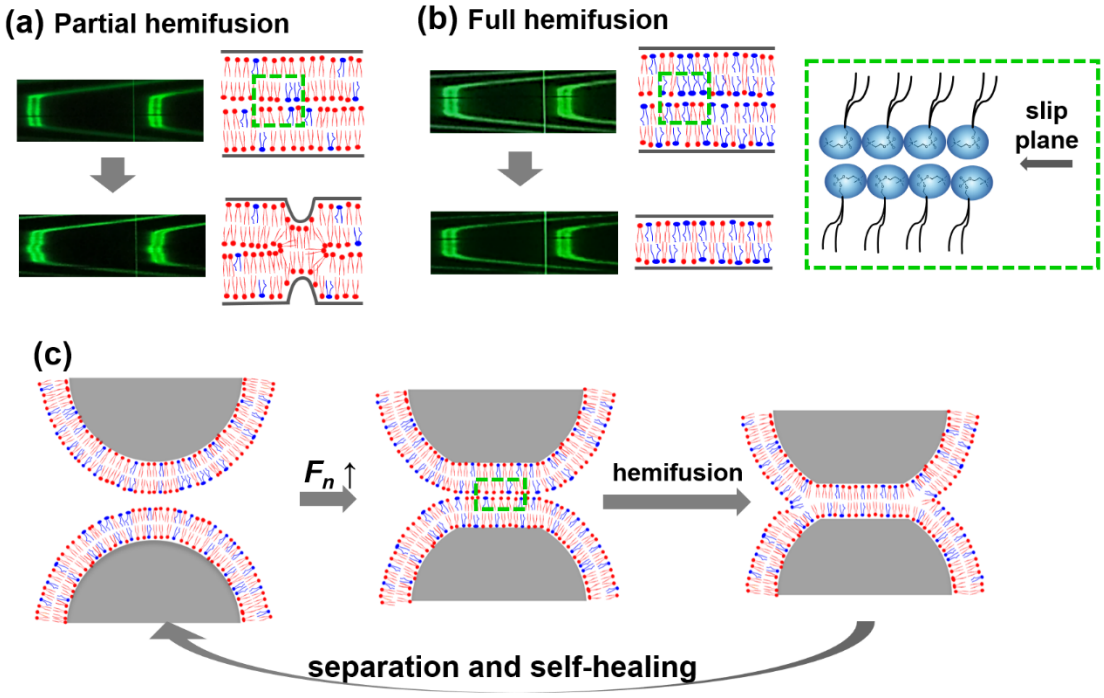

Figure 4. Typical shapes of multiple-beam interference fringes before (upper images) and after (lower images) partial (a) and full (b) hemifusion, and illustration (c) of two mica supported DPPC-POPC bilayers before contact, in close contact ('hard-wall'), after hemifusion, and subsequent separation and self-healing with reservoir to the original state. In (a) and (b), the vertical line of wavelength 546.1 nm was used as a reference during the measurements. The illustrations right to each fringe image show the structures of mica supported lipid bilayer(s), with DPPC and POPC molecules in yellow and blue colors (online), respectively. Dashed line squares show the slip-plane lying between two opposing layers of PC headgroups.

Receding force profiles. Receding profiles $F_n(D)$ were measured upon separating the mica-supported bilayers. From the results shown in Figures 3d-f, we can see that the receding and approaching profiles are not reversible. Repulsive forces between two bilayers on approaching were observed for all the three systems. However, attractive

forces (F_n < 0) and 'jumps-out' were observed for all the systems that experienced hemifusion. 'Jump-out' occurs on separation due to a Euler-like instability of the normal spring. For DPPC-POPC 8:2 bilayers that experienced partial hemifusion, jump-out took place at separation distance of 12.1 ± 0.7 nm, corresponding to the thickness of two extended bilayers. A jump-out to a separation 63.7 ± 16.3 nm was recorded. The corresponding pull-off force was -0.8 ± 0.2 mJ/m^2, intermediate between the van der Waals interaction between two PC bilayers of fluid-phase POPC (-0.6 mJ/m^2)[45] and gel-phase DPPC (-0.90 ± 0.15 mJ/m^2)[46]. In contrast, for the other two systems where full hemifusion occurred, the jump-out distances were 3.1 ± 0.5 μm and 2.1 ± 0.4 μm for 5:5 and 2:8, indicating much stronger adhesive forces than the van der Waals interaction. Detailed discussion is in the following section.

As shown in Figure 3, the normal force profiles obtained from independent experiments and different contact positions are generally repeatable. More interestingly, even after hemifusion, the normal force profiles of the second and following approaches (Figure 3, open/open with dot symbols) follow the similar trends as the first ones at the same contact positions for all the studied systems. This reproducibility of the normal force profiles implies that the two surfaces healed and each mica surface was covered by one lipid bilayer upon the approaches after hemifusion and separation (Figure 4c).

Frictional forces

Shear force traces were recorded while measuring the normal forces and surface separation distances. The typical applied lateral back-and-forth motion (top traces) and corresponding shear traces at different surface separation distances and pressures are

shown in Figure 5. The sliding friction force is measured from the plateau region of the shear-force traces. In Figure 5a, we can see that the sliding friction force between two DPPC-POPC 8:2 bilayers increased gradually until an abrupt increase in shear force took place, where no relative sliding between two surfaces was recorded and the surfaces moved rigidly together. This so-called 'rigid-coupling' happens when the applied lateral force is lower than the static friction force, so that there is no relative movement between the two surfaces. Similar phenomena were observed for DPPC-POPC 5:5 and 2:8, except for the fact that lower friction forces before 'rigid-coupling' were observed for the 5:5 system (Figure 5b), and even much lower shear forces (at the noise level) for the DPPC-POPC 2:8 (Figure 5c) prior to 'rigid-coupling'. Occasionally, 'shear to rigid-coupling' transitions, as shown in the bottom traces of Figures 5b-c, were recorded.

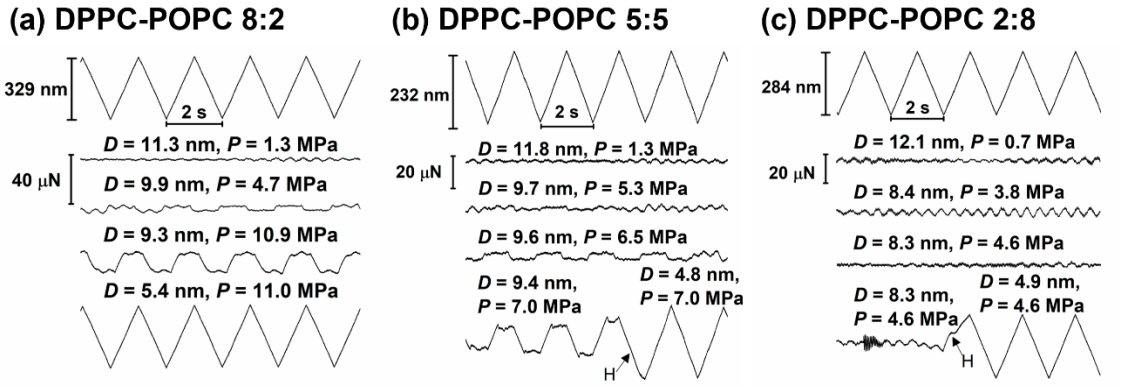

Figure 5. Typical shear traces for DPPC-POPC 8:2 (a), 5:5 (b), and 2:8 (c) at different separation distances (*D*) and pressures (*P*). The friction forces are evaluated through frequency analysis at the drive frequency. The top traces were lateral motion applied to the upper lens by PZT, the same as the lateral displacement of the bottom ones when 'rigid-coupling' occurs, which is accompanied by a decrease in *D*.

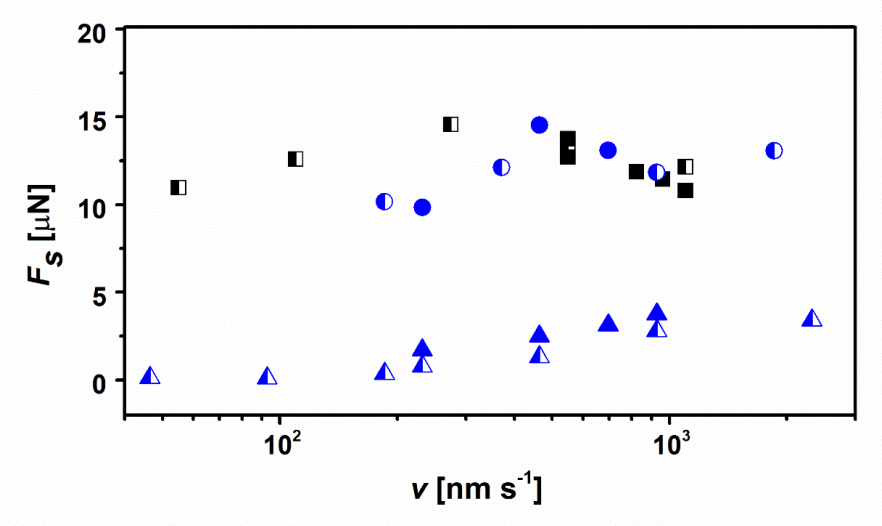

Figure 6. Shear force (F_s) as a function of sliding velocity (v_s) for DPPC-POPC 8:2 at D = 9.7 nm and pressure P = 5.24 MPa (squares), as well as DPPC-POPC 5:5 at D = 10.6 nm and P = 3.29 MPa (triangles, data obtained from the second approach) and D = 11.4 nm and P = 3.43 MPa (spheres, data obtained from the first approach of a different contact position from the triangles), immersed in 0.3 mM of the respective DPPC-POPC-SUV dispersions. The three sets of data were from independent experiments. The sliding velocity was adjusted by changing either the amplitude of lateral displacement at a given back-and-forth frequency (filled symbols), or the frequency at a fixed lateral displacement amplitude (half-filled symbols). The shear forces for DPPC-POPC 2:8 system are below the detection limit (a noise level of ca. 0.3 μN) before hemifusion occurs, so we couldn't get the accurate values and didn't report here.

The sliding friction forces F_s measured at different surface separations D and pressures as a function of the sliding velocity v_s are plotted in Figure 6. We note that F_s is largely independent of v_s over the range of parameters shown, clearly indicating a boundary lubrication mode for the mixed DPPC-POPC bilayers.

The variation of sliding friction forces with normal loads (F_s vs. F_n) are presented in Figure 7, and show that the friction coefficients μ for different DPPC-POPC mixtures are extremely low, $\mu \approx 10^{-4}$ or even lower, even under physiological-level contact stresses up to 3.2 – 10.9 MPa. For the DPPC-rich 8:2 system, μ was in the range of (2.2 – 5.0)

$\times 10^{-4}$ under pressures up to 8.5 – 10.9 MPa; while for the POPC-rich 2:8 system, friction coefficients lower than 10^{-4} were obtained at pressures ranging 4.6 – 5.9 MPa. For the system DPPC-POPC 5:5, friction coefficients of 1.8×10^{-3} – 2.3×10^{-4} under pressures of 3.2 – 7.7 MPa were obtained. Compared with single component PCs, where μ = (1.6 – 3.0) $\times 10^{-4}$ at pressures up to 18 MPa for DPPC and $\mu < 10^{-4}$ at pressures as high as 16 MPa were obtained.[15] the DPPC-rich system behaves more like a single component DPPC, and the POPC-rich system is like a single component POPC, while the DPPC-POPC 5:5 system shows higher friction coefficients before hemifusion occurs. The friction coefficients for the successive approaches were lower than the first ones, which is attributed to removal of loosely-attached liposomes on the surfaces, which result in viscoelastic dissipation when they are first sheared and removed, but then after removal on second and subsequent approaches this dissipation is reduced, hence lower friction.

A summary of the F_s vs. F_n variation for the three systems is shown in Figure 7d, from which we can see the 8:2 system sustains the highest normal forces and the 2:8 system exhibits the lowest shear forces prior to abrupt rigid-coupling of the two surfaces.

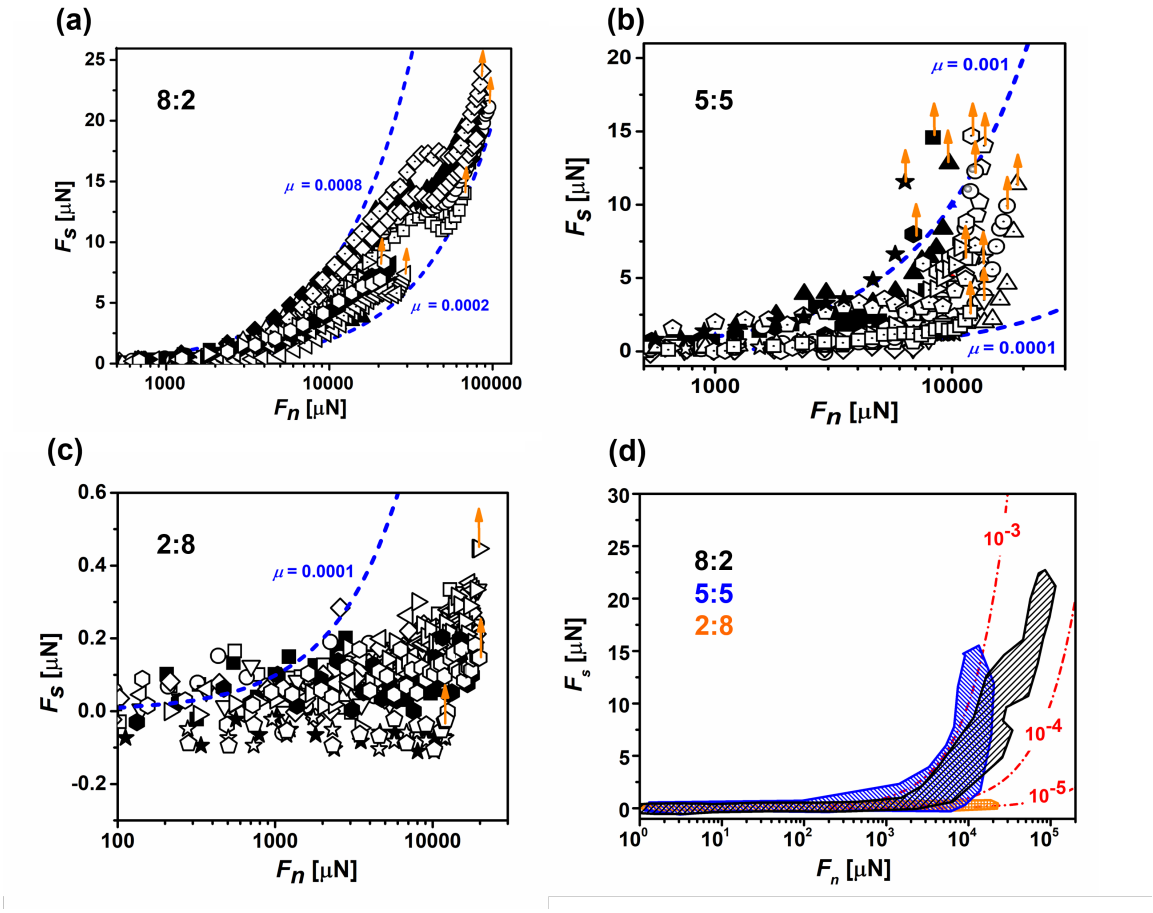

Figure 7. Shear force versus normal force for DPPC-POPC 8:2 (a), 5:5 (b), and 2:8 (c), immersed in 0.3 mM of the respective DPPC-POPC-SUV dispersions. The summary of all the three systems is shown in (d). The yellow arrows indicate abrupt increases in shear forces when 'rigid-coupling' was observed. The filled symbols represent the first approaches at different contact positions, while the empty/empty with dot ones represent the successive approaches. The friction coefficients (μ) and pressures (P) were calculated by the last data points before rigid-coupling/hemifusion.

The very low friction coefficients between two mica-supported, mixed DPPC-POPC bilayers is in agreement with the previous study that single-component PC vesicles/lipids exhibit excellent lubrication behavior by virtue of the hydration lubrication effect.[15,16,47] On one hand, the hydration layer surrounding the zwitterionic headgroups

(10 – 15 water molecules per headgroup[48,49]) reduces the energy dissipation by acting very fluidly when the slip-plane lies between two boundary PC layers, giving rise to low sliding friction forces; on the other hand, water molecules are bound tenaciously to the headgroups via charge-dipole interaction and thus can support strong repulsive forces, when the two surfaces are compressed, without being squeezed out. The resulting low friction at high normal loads leads to extremely low friction coefficients. Similarly to the DPPC-POPC 2:8 system, friction coefficients $< 10^{-4}$ have been reported for single-component DMPC and POPC bilayer coated mica surfaces across liposome dispersions at temperature higher than their phase transition temperatures.[15] This lubrication behavior is likely related to the liquid crystalline state of the bilayers: for PC molecules in liquid crystalline state, their higher hydration level and lower packing density than those in gel state, together with the ability to rapidly self-heal in the presence of the lipid reservoir in the SUV dispersions, give rise to reduced energy dissipation during sliding.[50,51,52]

An abrupt increase in the friction force was observed simultaneously with hemifusion, as indicated by the arrows in Figures 7a-c. We attribute this to the slip plane changing upon hemifusion. Following hemifusion, the slip plane between two opposing, highly-hydrated PC headgroups interfaces is replaced by a tail-tail interface at the midplane between the surfaces (Figure 4). Such an interface, dominated by van der Waals attraction between the hydrophobic lipid tails, is associated with much larger dissipation on sliding, hence much higher friction. Higher friction coefficients were also observed without reservoir of SUVs, under which condition the lipid bilayers might be discontinuous and unable to heal, and thus collapse under high load (Figure S4).

Hemifusion, Adhesion, and Self-healing

Hemifusion. Hemifusion has been widely recognized as an intermediate state of cell membrane fusion.[53] The involved stalk formation followed by reducing the inter-membrane distance can be triggered by SNARE or SM (Sec1/Munc18-like) proteins,[54] by intramembrane tension,[55] or by applying high normal pressures.[15] Packing mismatches and local defects in the supported bilayer are considered to be essential to induce hemifusion by exposing the hydrophobic tails, the long-ranged hydrophobic attraction between which overcomes the hydration repulsion and thereby leads to hemifusion.[56] Previous surface forces studies have reported hemifusion between mica-supported bilayers such as 1,2-dipalmitoyl-*sn*-glycero-3-phosphoethanolamine (DPPE),[57] 1,2-dimyristoyl-*sn*-glycero-3-phosphocholine (DMPC),[15] egg yolk PC,[56] and mixtures of DPPC-cholesterol[58].

For single-component phospholipid, defects on the bilayer are considered to be the main reason for hemifusion.[56] No hemifusion was observed for gel-state DPPC up to 18 MPa and for liquid crystalline-state POPC up to 16 MPa in the presence of the SUV dispersion.[15] In this study, high normal pressure together with the mismatch arising from mixed lipids is most likely the main reason for hemifusion. The thickness of two supported bilayers before and after hemifusion (left and middle columns in each trio), as well as the thickness change on hemifusion (ΔD, right column in trio), versus POPC content in the system, is shown in Figure 8. The thickness of two removed proximal/outer leaflets (~ 4 nm) appears thinner than the remaining two cytoplasmic/inner leaflets (~ 5 nm), indicating the bilayers deformed elastically by thinning under high pressures (about

5 ~ 10 MPa). For the mixed PC lipids system, the packing mismatches of DPPC and POPC presumably reduce the energy barrier and facilitates hemifusion.

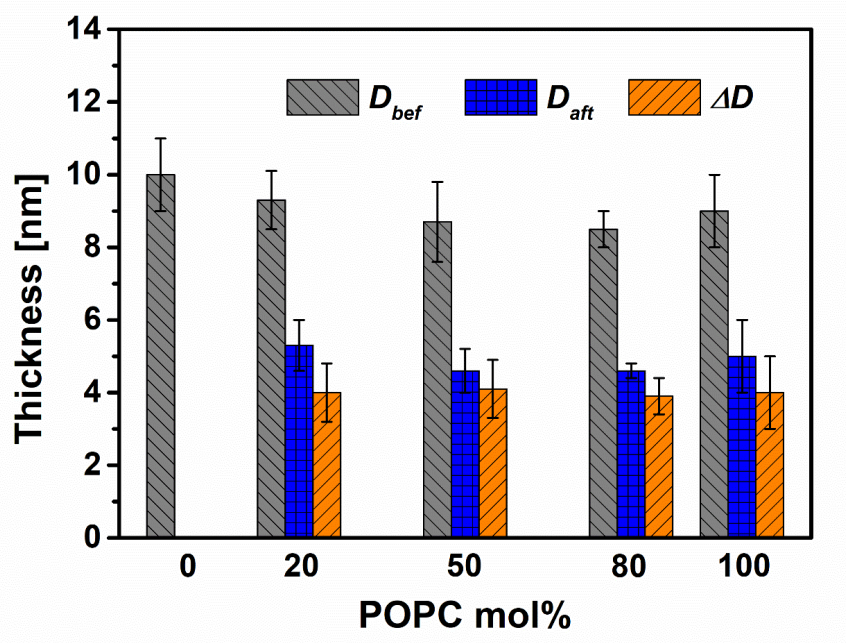

Figure 8. The surface separation distances between two mica surfaces before (D_{bef}) and after (D_{aft}) hemifusion as well as the change in thickness (ΔD) upon hemifusion versus the molar fraction of POPC in the mixtures. Thicknesses of two compressed bilayers D_{bef} before and single bilayer D_{aft} after hemifusion are 9.3 ± 0.8 nm and 5.3 ± 0.7 nm (n = 19), 8.7 ± 1.1 nm and 4.6 ± 0.6 nm (n = 16), and 8.5 ± 0.5 nm and 4.6 ± 0.2 nm (n = 12) for 20%, 50%, and 80% POPC, respectively, where the ± indicates standard deviations. The data for pure DPPC (POPC mol% = 0, D_{bef} = 10 ± 1 nm) and POPC (D_{bef} = 10 ± 1 nm, D_{aft} = 5 ± 1 nm) were adapted from Ref. 15. No hemifusion was observed between gel-state DPPC bilayers.

For DPPC-POPC 5:5 and 2:8, where the mixtures are mainly in liquid crystalline state according to the measured main phase transition temperatures of these mixtures (see Figure S2), fully hemifused contact regions were observed. As for DPPC-POPC 8:2 mixtures, where partial hemifusion and phase separation of supported bilayer on mica

was indicated (Figure 2), we suspect that the DPPC-rich domains did not undergo hemifusion (Figure 4a) owning to the fact that the gel state DPPC-rich area is robust enough to sustain such high pressures in the presence of reservior.[15] Therefore, the gel state PC domains are expected to play a dominant role in preventing the hemifusion from happening under physiological pressures.

Adhesion. The interfacial adhesion energy (γ) was calculated according to the Johnson-Kendall-Roberts (JKR) model and the results are listed in Table 1. Under conditions that a PC bilayer is trapped between two mica surfaces, the interfacial energies for DPPC-POPC 8:2, 5:5 and 2:8 are in a decreasing trend of -6.74 ± 1.24, -4.90 ± 0.80, and -3.30 ± 0.60 mJ/m^2, respectively. These values are much lower than the alkane-water interfacial energy (-50 mJ/m^2),[59] but are comparable to the value obtained for interfaces of HSPC-mica (-14 ± 4 mJ/m^2),[17] HSPC-40% cholesterol/mica (- 10.5 ± 4.3 mJ/m^2) and DMPC-40% cholesterol/mica (~ 4 mJ/m^2)[58]. Therefore, we may conclude that the interface upon separation is not the hydrophobic tail/tail interface, but the PC headgroups/mica interface. From Table 1, we can also see that the interfacial energy is related to the phase transition temperature of the PC lipids. Generally, for PC lipids with higher T_m, the headgroup-mica interaction strength is stronger due to the lower area per lipid,[42] and vice versa.

Table 1. Interfacial energy calculated from separating between two mica surfaces with a trapped bilayer in between.

systems	**γ/(mJ/m^2)**
alkane-water[59]	~ -50
HSPC-mica (in water)[17]	-14 ± 4*
HSPC-40% cholesterol (in bulk) [58]	-10.5 ± 4.3
DPPC-POPC 8:2-mica (in water)	-6.74 ± 1.24*
DPPC-POPC 5:5 (in bulk)	-4.90 ± 0.80
DMPC-40% cholesterol (in bulk) [58]	~ -4
DPPC-POPC 2:8 (in bulk)	-3.30 ± 0.60
POPC (in bulk)	-2.29 ± 0.25**

*For the HSPC and DPPC-POPC 8:2 systems, no hemifusion was observed in SUV dispersion, where two surfaces were both coated with gel-state SUVs or bilayers. The interfacial energies were measured with an asymmetric system consisting a bare mica surface and a PC bilayer-coated mica surface across water.
**The interfacial energy was calculated according to a separate experiment where hemifusion took place.

Self-healing. Self-maintenance of the boundary lubricant upon sliding is crucial to maintain low friction coefficients and prevent the underlying matrix from wearing. Since the separation plane, deduced from γ values lies in the PC headgroup - mica interface, on separation from hemifusion one surface is bare mica, the other is coated by the bilayer. Reproducible normal force profiles obtained in the successive approaches, following hemifusion and separation, indicate rapid self-healing of the boundary bilayers by PC molecules in the reservoir (illustrated in Figure 4c). This was further support by the fact that higher friction under lower load for DPPC-POPC 8:2 bilayer coated surfaces under

water than across SUV dispersion (Figure S4). This may have bearing in the context of biolubrication of synovial joints, where high friction coefficients between articular cartilages could be correlated with the onset of osteoarthritis, a widespread joint disease which is associated with cartilage wear.[28] Previous studies have shown that the self-healing of PC lipids is related to their fluidity: fast self-healing of DMPC bilayers was observed,[15] however, healing of a bilayer composed of DPPE supported 1,2-dilauroyl-*sn*-glycero-3-phosphoethanolamine (DLPE) takes hours to days.[57] In the present work, the unsaturated PC may play a key role in rapid self-healing and maintaining the integrity of the boundary bilayer, which lowers the friction and protects the underlying layers. This finding suggests that the abundant unsaturated PCs in human synovial fluid may be of great importance in maintaining the integrity of boundary PC layers on the cartilage surface and in transferring phospholipid from synovial fluid to the cartilage surfaces to heal disrupted bilayers, thereby lowing the friction and protecting the underlying layers from wear.

■ CONCLUSIONS

Normal and shear forces between DPPC-POPC (8:2, 5:5, and 2:8, molar ratios)-coated mica surfaces were measured using an SFB across dispersions of the respective SUVs. On approaching, short ranged (D ~ 10 nm) repulsion between the opposing DPPC-POPC bilayers was observed at the highest compressions attained. Meanwhile, extremely low friction coefficients of 10^{-4} level or even lower under pressures of up to 3.2 – 10.9 MPa were also obtained, attributed to the hydration lubrication mechanism. At higher pressures hemifusion and a sharp rise in friction was seen. Among the three studied

systems, the DPPC-rich system (8:2) is able to sustain highest pressure (8.5 – 10.9 MPa) prior to hemifusion, while the POPC-rich system (2:8) maintains the lowest friction coefficient (< 10^{-4}) prior to hemifusion. Hemifusion induced at a critical pressure was found over the whole contact region for the DPPC-POPC 5:5 and 2:8 mixtures, possibly due to the packing mismatches of two PC components; while partial hemifusion occurred for DPPC-POPC 8:2 bilayers, where the robust gel state DPPC-rich domains can sustain higher pressures and so do not hemifuse. Upon separating the hemifused bilayers supported by two mica surfaces, adhesive attraction was recorded. The surface tension was calculated from pull-off forces, indicating that the separation plane lies in the PC headgroup plane-mica interface. Since such separation is expected to leave each mica surface partly bare and partly coated by a bilayer, the fact that in the successive approaches, following hemifusion and separation, reproducible normal force profiles were obtained, indicate rapid self-healing of the supported bilayers by PC molecules in the reservoir. This study provides insight and is a first step to understanding how the multi-component PC (and other) lipids present in articular joints may affect cartilage boundary lubrication, which is attributed to lipid-exposing boundary layers on the articular surface, and to designing more efficient lipid-based boundary biolubricants.

■ ASSOCIATED CONTENT

Supporting Information

The Supporting Information is available free of charge on the ACS Publications website.

1. Results on the characterization of prepared DPPC-POPC-SUVs with DLS; 2. zeta potentials of liposomes used; 3. ^{1}H-NMR, ^{31}P-NMR; 4. DSC results; 5. force profiles for opposing DPPC-POPC 8:2 bilayers under water.

■ AUTHOR INFORMATION

Corresponding Author

*E-mail: jacob.klein@weizmann.ac.il

Notes

The authors declare no competing financial interest.

■ ACKNOWLEDGEMENTS

The authors would like to thank Dr. Weifeng Lin and Dr. Ran Tivony for helpful discussions. This research was supported by the European Research Council (Advanced Grant CartiLube), by the McCutchen Foundation, by the Israel Science Foundation – National Natural Science Foundation of China joint research Program (Grant 2577/17), and was made possible in part by the historic generosity of the Harold Perlman family.

■ REFERENCES

(1) Van Meer, G.; Voelker, D. R.; Feigenson, G. W. Membrane Lipids: Where They Are and How They Behave. *Nat. Rev. Mol. Cell Biol.* **2008**, *9* (2), 112–124. https://doi.org/10.1038/nrm2330.

(2) Kosinska, M. K.; Liebisch, G.; Lochnit, G.; Wilhelm, J.; Klein, H.; Kaesser, U.; Lasczkowski, G.; Rickert, M.; Schmitz, G.; Steinmeyer, J. A Lipidomic Study of Phospholipid Classes and Species in Human Synovial Fluid. *Arthritis Rheum.* **2013**, *65* (9), 2323–2333. https://doi.org/10.1002/art.38053.

(3) Sarma, A. V; Powell, G. L.; LaBerge, M. Phospholipid Composition of Articular Cartilage Boundary Lubricant. *J. Orthop. Res.* **2001**, *19*, 671–676. https://doi.org/10.1016/S0736-0266(00)00064-4.

(4) Callan-Jones, A.; Sorre, B.; Bassereau, P. Curvature-Driven Lipid Sorting in Biomembranes. *Cold Spring Harb. Perspect. Biol.* **2011**, *3* (2), 1–14. https://doi.org/10.1101/cshperspect.a004648.

(5) Jahn, S.; Klein, J. Hydration Lubrication: The Macromolecular Domain. *Macromolecules* **2015**, *48* (15), 5059–5075. https://doi.org/10.1021/acs.macromol.5b00327.

(6) Chen, Y.; Hills, B. A.; Hills, Y. C. Unsaturated Phosphatidylcholine and Its Application in Surgical Adhesion. *ANZ J. Surg.* **2005**, *75* (12), 1111–1114. https://doi.org/10.1111/j.1445-2197.2005.03619.x.

(7) Forster, H.; Fisher, J. The Influence of Loading Time and Lubricant on the Friction of Articular Cartilage. *Proc. Inst. Mech. Eng. H.* **1996**, *210* (2), 109–119. https://doi.org/10.1243/PIME_PROC_1996_210_399_02.

(8) Adams, D.; Swanson, S. A. Direct Measurement of Local Pressures in the Cadaveric Human Hip Joint during Simulated Level Walking. *Ann Rheum Dis.* **1985**, *44*, 658–666. https://doi.org/10.1136/ard.44.10.658.

(9) Hodge, W. A.; Fijan, R. S.; Carlson, K. L.; Burgess, R. G.; Harris, W. H.; Mann, R. W. Contact Pressures in the Human Hip Joint Measured in Vivo. *Proc. Natl. Acad. Sci.* **1986**, *83* (9), 2879–2883. https://doi.org/10.1073/pnas.83.9.2879.

(10) Ozturk, H. E.; Stoffel, K. K.; Jones, C. F.; Stachowiak, G. W. The Effect of Surface-Active Phospholipids on the Lubrication of Osteoarthritic Sheep Knee Joints: Friction. *Tribol. Lett.* **2004**, *16* (4), 283–290. https://doi.org/10.1023/B:TRIL.0000015204.41674.d3.

(11) Duan, Y.; Liu, Y.; Li, J.; Feng, S.; Wen, S. AFM Study on Superlubricity between Ti6Al4V/Polymer Surfaces Achieved with Liposomes. *Biomacromolecules* **2019**, *20* (4),

1522–1529. https://doi.org/10.1021/acs.biomac.8b01683.

(12) Zheng, R.; Arora, J.; Boonkaew, B.; Raghavan, S. R.; Kaplan, D. L.; He, J.; Pesika, N. S.; John, V. T. Liposomes Tethered to a Biopolymer Film through the Hydrophobic Effect Create a Highly Effective Lubricating Surface. *Soft Matter* **2014**, *10* (46), 9226–9229. https://doi.org/10.1039/C4SM01692K.

(13) Trunfio-Sfarghiu, A. M.; Berthier, Y.; Meurisse, M. H.; Rieu, J. P. Multiscale Analysis of the Tribological Role of the Molecular Assemblies of Synovial Fluid. Case of a Healthy Joint and Implants. *Tribol. Int.* **2007**, *40* (10–12), 1500–1515. https://doi.org/10.1016/j.triboint.2007.02.008.

(14) Wang, M.; Zander, T.; Liu, X.; Liu, C.; Raj, A.; Wieland, D. C. F.; Garamus, V. M.; Willumeit-römer, R.; Martin, P.; De, A. The Effect of Temperature on Supported Dipalmitoylphosphatidylcholine (DPPC) Bilayers: Structure and Lubrication Performance. *J. Colloid Interf. Sci.* **2015**, *445*, 84–92. https://doi.org/10.1016/j.jcis.2014.12.042.

(15) Sorkin, R.; Kampf, N.; Zhu, L.; Klein, J. Hydration Lubrication and Shear-Induced Self-Healing of Lipid Bilayer Boundary Lubricants in Phosphatidylcholine Dispersions. *Soft Matter* **2016**, *12* (10), 2773–2784. https://doi.org/10.1039/C5SM02475G.

(16) Sorkin, R.; Kampf, N.; Dror, Y.; Shimoni, E.; Klein, J. Origins of Extreme Boundary Lubrication by Phosphatidylcholine Liposomes. *Biomaterials* **2013**, *34* (22), 5465–5475. https://doi.org/10.1016/j.biomaterials.2013.03.098.

(17) Goldberg, R.; Schroeder, A.; Silbert, G.; Turjeman, K.; Barenholz, Y.; Klein, J. Boundary Lubricants with Exceptionally Low Friction Coefficients Based on 2D Close-Packed Phosphatidylcholine Liposomes. *Adv. Mater.* **2011**, *23* (31), 3517–3521. https://doi.org/10.1002/adma.201101053.

(18) Zhu, L.; Seror, J.; Day, A. J.; Kampf, N.; Klein, J. Ultra-Low Friction between Boundary Layers of Hyaluronan-Phosphatidylcholine Complexes. *Acta Biomater.* **2017**, *59*, 283–292. https://doi.org/10.1016/j.actbio.2017.06.043.

(19) Raviv, U.; Klein, J. Fluidity of Bound Hydration Layers. *Science.* **2002**, *297*, 1540–1543. https://doi.org/10.1126/science.1074481.

(20) Klein, J. Hydration Lubrication. *Friction* **2013**, *1* (1), 1–23. https://doi.org/10.1007/s40544-013-0001-7.

(21) Ma, L.; Gaisinskaya-Kipnis, A.; Kampf, N.; Klein, J. Origins of Hydration Lubrication. *Nat. Commun.* **2015**, *6*, 6060. https://doi.org/10.1038/ncomms7060.

(22) Li, J.; Zhang, C.; Sun, L.; Lu, X.; Luo, J. Tribochemistry and Superlubricity Induced by Hydrogen Ions. *Langmuir* **2012**, *28* (45), 15816–15823. https://doi.org/10.1021/la303897x.

(23) Kampf, N.; Wu, C.; Wang, Y.; Klein, J. A Trimeric Surfactant: Surface Micelles, Hydration-Lubrication, and Formation of a Stable, Charged Hydrophobic Monolayer. *Langmuir* **2016**, *32* (45), 11754–11762. https://doi.org/10.1021/acs.langmuir.6b02657.

(24) Chen, M.; Briscoe, W. H.; Armes, S. P.; Klein, J. Lubrication at Physiological Pressures by Polyzwitterionic Brushes. *Science* **2009**, *323* (5922), 1698–1701. https://doi.org/10.1126/science.1169399.

(25) Seror, J.; Merkher, Y.; Kampf, N.; Collinson, L.; Day, A. J.; Maroudas, A.; Klein, J. Normal and Shear Interactions between Hyaluronan − Aggrecan Complexes Mimicking Possible Boundary Lubricants in Articular Cartilage in Synovial Joints. *Biomacromolecules* **2012**, *13*, 3823–3832. https://doi.org/10.1021/bm301283f.

(26) Das, S.; Banquy, X.; Zappone, B.; Greene, G. W.; Jay, G. D.; Israelachvili, J. N. Synergistic Interactions between Grafted Hyaluronic Acid and Lubricin Provide Enhanced Wear Protection and Lubrication. *Biomacromolecules* **2013**, *14* (5), 1669–1677. https://doi.org/10.1021/bm400327a.

(27) Seror, J.; Zhu, L.; Goldberg, R.; Day, A. J.; Klein, J. Supramolecular Synergy in the Boundary Lubrication of Synovial Joints. *Nat. Commun.* **2015**, *6*, 6497. https://doi.org/10.1038/ncomms7497.

(28) Jahn, S.; Seror, J.; Klein, J. Lubrication of Articular Cartilage. *Annu. Rev. Biomed. Eng.* **2016**, *18* (1), 235–258. https://doi.org/10.1146/annurev-bioeng-081514-123305.

(29) Chen, Y.; Crawford, R. W.; Oloyede, A. Unsaturated Phosphatidylcholines Lining on the Surface of Cartilage and Its Possible Physiological Roles. *J. Orthop. Surg. Res.* **2007**, *2*, 14. https://doi.org/10.1186/1749-799X-2-14.

(30) Kosinska, M. K. Boundary Lubricants in Osteoarthritic Synovial Fluid, Ph.D. Dissertation, Justus-Liebig University Giessen, 2012.

(31) Klein, J.; Kumacheva, E. Simple Liquids Confined to Molecularly Thin Layers. I. Confinement-Induced Liquid-to-Solid Phase Transitions. *J. Chem. Phys.* **1998**, *108* (16), 6996. https://doi.org/10.1063/1.476114.

(32) Tabor, D.; Winterton, R. H. S. The Direct Measurement of Normal and Retarded van Der Waals Forces. *Proc. Roy. Soc. A.* **1969**, *312*, 435–450. https://doi.org/https://doi.org/10.1098/rspa.1969.0169.

(33) Johnson, K. L.; Kendall, K.; Roberts, A. D. Surface Energy and the Contact of Elastic Solids. *Proc. Roy. Soc. A.* **1971**, *324*, 301–313. https://doi.org/10.1098/rspa.1971.0141.

(34) Jousma, H.; Talsma, H.; Spies, F.; Joosten, J. G. H.; Junginger, H. E.; Crommelin, D. J. A. Characterization of Liposomes. The Influence of Extrusion of Multilamellar Vesicles

through Polycarbonate Membranes on Particle Size, Particle Size Distribution and Number of Bilayers. *Int. J. Pharm.* **1987**, *35* (3), 263–274. https://doi.org/10.1016/0378-5173(87)90139-6.

(35) Fuchs, B.; Schiller, J.; Wagner, U.; Häntzschel, H.; Arnold, K. The Phosphatidylcholine/ Lysophosphatidylcholine Ratio in Human Plasma Is an Indicator of the Severity of Rheumatoid Arthritis: Investigations by ^{31}P NMR and MALDI-TOF MS. *Clin. Biochem.* **2005**, *38*, 925–933. https://doi.org/10.1016/j.clinbiochem.2005.06.006.

(36) Metso, A. J.; Zhao, H.; Tuunainen, I.; Kinnunen, P. K. J. Observation of the Main Phase Transition of Dinervonoylphosphocholine Giant Liposomes by Fluorescence Microscopy. *Biochim. Biophys. Acta* **2005**, *1713*, 83–91. https://doi.org/10.1016/j.bbamem.2005.04.011.

(37) Åkesson, A.; Lind, T.; Ehrlich, N.; Stamou, D.; Wacklin, H.; Cárdenas, M. Composition and Structure of Mixed Phospholipid Supported Bilayers Formed by POPC and DPPC. *Soft Matter* **2012**, *8* (20), 5658. https://doi.org/10.1039/c2sm00013j.

(38) Giocondi, M. C.; Yamamoto, D.; Lesniewska, E.; Milhiet, P. E.; Ando, T.; Le Grimellec, C. Surface Topography of Membrane Domains. *Biochim. Biophys. Acta - Biomembr.* **2010**, *1798* (4), 703–718. https://doi.org/10.1016/j.bbamem.2009.09.015.

(39) Oguchi, T.; Sakai, K.; Sakai, H.; Abe, M. DSPC/DLPC Mixed Films Supported on Silica: A QCM-D and Friction Force Study. *J. Oleo Sci.* **2011**, *60* (4), 177–183. https://doi.org/10.5650/jos.60.177.

(40) Raviv, U.; Laurat, P.; Klein, J. Fluidity of Water Confined to Subnanometre Films. *Nature* **2001**, *413*, 51–54. https://doi.org/https://doi.org/10.1038/35092523.

(41) Janiak, M. J.; Small, D. M.; Shipley, G. G. Nature of the Thermal Pretransition of Synthetic Phospholipids: Dimyristoyl- and Dipalmitoyllecithin. *Biochemistry* **1976**, *15* (21), 4575–4580. https://doi.org/10.1021/bi00666a005.

(42) Kučerka, N.; Nieh, M. P.; Katsaras, J. Fluid Phase Lipid Areas and Bilayer Thicknesses of Commonly Used Phosphatidylcholines as a Function of Temperature. *Biochim. Biophys. Acta - Biomembr.* **2011**, *1808* (11), 2761–2771. https://doi.org/10.1016/j.bbamem.2011.07.022.

(43) Disalvo, E. A.; Lairion, F.; Martini, F.; Tymczyszyn, E.; Frías, M.; Almaleck, H.; Gordillo, G. J. Structural and Functional Properties of Hydration and Confined Water in Membrane Interfaces. *Biochim. Biophys. Acta - Biomembr.* **2008**, *1778* (12), 2655–2670. https://doi.org/10.1016/j.bbamem.2008.08.025.

(44) Horn, R. G. Direct Measurement of the Force between Two Lipid Bilayers and Observation of Their Fusion. *Biochim. Biophys. Acta - Biomembr.* **1984**, *778*, 224–228.

https://doi.org/https://doi.org/10.1016/0005-2736(84)90466-8.

(45) Marra, J.; Israelachvili, J. Direct Measurements of Forces between Phosphatidylcholine and Phosphatidylethanolamine Bilayers in Aqueous Electrolyte Solutions. *Biochemistry* **1985**, *24*, 4608–4646. https://doi.org/10.1021/bi00338a020.

(46) Marra, J. Direct Measurements of Attractive van Der Waals and Adhesion Forces between Uncharged Lipid Bilayers in Aqueous Solutions. *J. Colloid Interface Sci.* **1986**, *109* (1), 11–20. https://doi.org/https://doi.org/10.1016/0021-9797(86)90276-6.

(47) Li, J.; Cao, W.; Wang, Z.; Ma, M.; Luo, J. Origin of Hydration Lubrication of Zwitterions on Graphene. Nanoscale 2018, 10 (35), 16887–16894. https://doi.org/10.1039/c8nr05724a.

(48) Wiener, M. C.; Suter, R. M.; Nagle, J. F. Structure of the Fully Hydrated Gel Phase of Dipalmitoylphosphatidylcholine. *Biophys. J.* **1989**, *55* (2), 315–325. https://doi.org/10.1016/S0006-3495(89)82807-3.

(49) Kučerka, N.; Tristram-Nagle, S.; Nagle, J. F. Structure of Fully Hydrated Fluid Phase Lipid Bilayers with Monounsaturated Chains. *J. Membr. Biol.* **2006**, *208* (3), 193–202. https://doi.org/10.1007/s00232-005-7006-8.

(50) Jendrasiak, G. L.; Hasty, J. H. The Hydration of Phospholipids. *Biochim. Biophys. Acta* **1974**, *337*, 79–91. https://doi.org/https://doi.org/10.1016/0005-2760(74)90042-3.

(51) Nagle, J. F.; Pan, J.; Tristram-nagle, S.; Kuc, N. Temperature Dependence of Structure , Bending Rigidity , and Bilayer Interactions of Dioleoylphosphatidylcholine Bilayers. *Biophys. J.* **2008**, *94* (1), 117–124. https://doi.org/10.1529/biophysj.107.115691.

(52) Poger, D.; Mark, A. E. On the Validation of Molecular Dynamics Simulations of Saturated and Cis -Monounsaturated Phosphatidylcholine Lipid Bilayers: A Comparison with Experiment. *J Chem Theory Comput* **2010**, *6* (1), 325–336. https://doi.org/10.1021/ct900487a.

(53) Chernomordik, L. V.; Kozlov, M. M. Mechanics of Membrane Fusion. *Nat. Struct. Mol. Biol.* **2008**, *15* (7), 675–683. https://doi.org/10.1038/nsmb.1455.

(54) TSüdhof, T. C.; Rothman, J. E. Membrane Fusion: Grappling with SNARE and SM Proteins. *Science* **2009**, *474*, 474–478. https://doi.org/10.1126/science.1161748.

(55) Hed, G.; Safran, S. A. Initiation and Dynamics of Hemifusion in Lipid Bilayers. *Biophys. J.* **2003**, *85* (1), 381–389. https://doi.org/10.1016/S0006-3495(03)74482-8.

(56) Helm, C. A.; Israelachvili, J. N.; Mcguiggans, P. M. Role of Hydrophobic Forces in Bilayer Adhesion and Fusion. *Biochemistry* **1992**, *31* (6), 1794–1805. https://doi.org/10.1021/bi00121a030.

(57) Benz, M.; Gutsmann, T.; Chen, N.; Tadmor, R.; Israelachvili, J. Correlation of AFM and

SFA Measurements Concerning the Stability of Supported Lipid Bilayers. *Biophys. J.* **2004**, *86* (2), 870–879. https://doi.org/10.1016/S0006-3495(04)74162-4.

(58) Sorkin, R.; Kampf, N.; Klein, J. Effect of Cholesterol on the Stability and Lubrication Efficiency of Phosphatidylcholine Surface Layers. *Langmuir* **2017**, *33*, 7459–7467. https://doi.org/10.1021/acs.langmuir.7b01521.

(59) Zeppieri, S.; Rodriguez, J.; de Ramos, A. L. L. Interfacial Tension of Alkane plus Water Systems. *J. Chem. Eng. Data* **2001**, *46* (5), 1086–1088. https://doi.org/10.1021/je000245r.

Table of Contents